

# DEVELOPMENT OF ITERATIVE LEARNING AND DISTURBANCE OBSERVER-BASED LLRF CONTROL SYSTEM FOR INTERNATIONAL LINEAR COLLIDER

Feng Qiu\*, Shinichiro Michizono, Toshihiro Matsumoto, Takako Miura,  
KEK, 1-1 Oho, Tsukuba, Ibaraki 305-0801, Japan  
Sigit Basuki Wibowo, Na Liu  
The Graduate School for Advanced Studies, Kanagawa 240-0193, Japan

## Abstract

This paper shows the development of a iterative learning control (ILC) combined with a disturbance observer (DOB)-based control for the digital low-level radio-frequency (LLRF) system of international linear collider (ILC) project. The motivation of this study is to compensate for the repetitive (or predictable) and unpredictable disturbances in the radio-frequency (RF) system such as beam loading, Lorentz force detuning (LFD) and microphonics. Results in a cavity simulator-based test bench demonstrate the possibility of the presented control approach. We have a plan to further generalize this approach to LLRF systems at superconducting test facility (STF) and future ILC project.

## INTRODUCTION

The International Linear Collider (ILC) is an proposed electron and positron collider facility for precisely investigating the Higgs boson, dark matter, and possible extra dimensions. A total of 400 radio frequency (RF) stations, each was equipped with 39 superconducting (SC) RF cavities driven by a 10 MW multi-beam klystron, will be established in ILC [1]. These cavities are operated in the pulse mode with 1.65 ms pulse duration, and 5 Hz repetition rate. The particle beam is then accelerated by the high gradient RF field in the RF cavities. In order to achieve high beam quality, the RF field fluctuation should be maintained at less than 0.07% (RMS) for the amplitude and 0.35° (RMS) for the phase, respectively [1]. In accelerators, LLRF systems are applied to stabilize the RF field.

The LLRF systems in a pulse mode machine are disturbed by various of disturbances [2]. Typical disturbances are classified into two categories: repetitive (or predictable) disturbances and unpredictable disturbances. Repetitive disturbances such as Lorentz force detuning (LFD) and beam-loading, are repeated in the system with 200 ms period. The unpredictable disturbances such as microphonics varies from pulse to pulse.

The repetitive disturbances can be removed by iterative learning control (ILC) [3–5]. In this control strategy, the error information gathered from the last cycles was estimated and used to improve the current cycle. ILC algorithm requires the system to perform the same action over and over again with high precision. This requirement can be fulfilled in a pulse mode operation accelerators such as ILC facility

and KEK superconducting test facility (STF) [6]. However, ILC algorithm is incapable of reject the unpredictable disturbances such as microphonics. In view of this situation, disturbance observer (DOB) based control method is introduced to suppress the microphonics effects. DOB control was successfully applied in the LLRF system of the compact energy recovery linac (cERL) test facility at KEK [2]. It is proved that the DOB control is effective for both repetitive and unpredictable disturbances. This motivate us to design a control algorithm which combined the advantages of ILC and DOB, and both of the repetitive and unpredictable errors are expected to be canceled in the combined control approach.

## ITERATIVE LEARNING CONTROL

ILC algorithms were originally developed for robot learning and training in [7]. Considering a discrete-time system  $G_p$  in the  $j$ -th trial

$$\begin{cases} x_j(k+1) = Ax_j(k) + Bu_j(k) \\ y_j(k) = Cx_j(k) \end{cases} \quad (1)$$

Here, the matrices A, B, and C describing the discrete-time system in the state space and  $x_j(k)$ ,  $u_j(k)$ , and  $y_j(k)$  are the state, control, and output variables, respectively. The subscript "j" and "k" represents the iteration index and time index, respectively.

A widely used ILC learning algorithm is given by

$$u_{j+1}(k) = Q_{ILC} [u_j(k) + L(e_j(k))] \quad (2)$$

Here,  $Q_{ILC}$  and  $L$  are defined as  $Q$ -filter and learning function, respectively. The signal  $e_j$  represents the error signal.

Figure 1 has illustrated the learning process of the ILC algorithm used in a LLRF system with pulse mode operation (e.g. LLRF system at ILC project). The learning process of ILC algorithm is illustrated in Fig. 1. In the  $j$ -th trial, the cavity error signal  $e_j(k)$ , is learned by the learning function  $L$ . The result  $L(e_j)$ , is added to the  $j$ -th control signal,  $u_j(k)$ . The combined signal is filtered by  $Q_{ILC}$  to enhance the robustness of the algorithm. The output signal is then updated by the filtered signal. In the  $j+1$  th trial, the cavity signal is detected at first, and then is compared with the given reference signal  $r$  to calculate the new error signal,  $e_{j+1}(k)$ . This algorithm is repeated from pulse to pulse, and the tracking accuracy is improved in this iterative process.

\* qiufeng@post.kek.jp

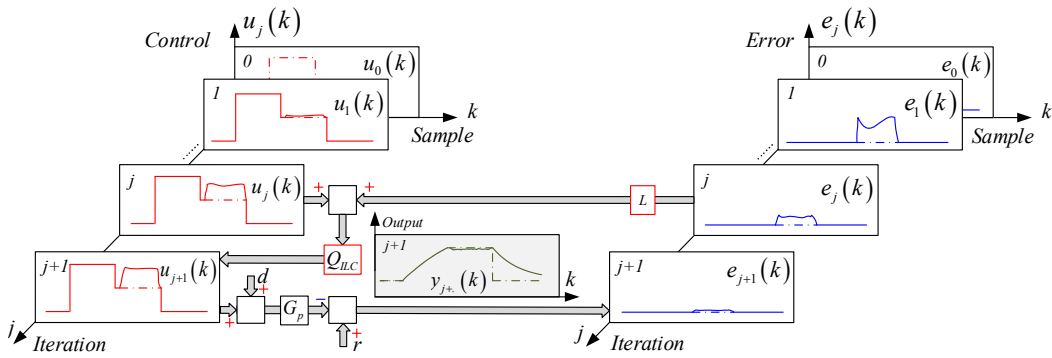


Figure 1: Learning process of ILC algorithm.

The simplest way is to defined  $L$  in (2), as a proportional gain  $k_p$ . In this case, the learning updated algorithm in (2) is simplified by

$$u_{j+1}(k) = Q_{ILC} [u_j(k) + k_p e_j(k)] . \quad (3)$$

Algorithm shown in (3) is also named P-type ILC. In our study, we have applied a P-type ILC at first because its ease of design and implementation. Many advanced ILC algorithms have been proposed including higher order ILC (HOILC),  $H_\infty$ -based ILC, plant inversion-based ILC and optimization-based ILC [3–5]. In our paper, we have selected the plant inversion-based ILC algorithm due to its fast convergence rate. The algorithm of plant inversion-based ILC can be expressed by

$$u_{j+1}(k) = Q_{ILC} [u_j(k) + G_n^{-1} e_j(k)] . \quad (4)$$

Here,  $G_n$  represents the nominal model of the actual system  $G_p$ . The learning function in this case is  $L = G_n^{-1}$ . Furthermore, to avoid the model uncertainty and enhance the robustness, a low-pass  $Q_{ILC}$  is employed.

### DOB-BASED CONTROL

DOB control was originally proposed in [8]. The disturbance observer is capable to estimate the repetitive and unpredictable disturbances of the system. If the estimated disturbances is with high accuracy, it is possible to cancel the real disturbances with the estimate. The structure of the DOB control is shown in Fig 2. Signals  $c$ ,  $\varepsilon$ ,  $d$ , and  $\hat{d}$  represent the control, plant input, disturbance, and disturbance estimate, respectively. Models  $G_p$  and  $G_n$  represent the transfer function of the real system and nominal system model ( $G_n \approx G_p$ ). The  $Q$ -filter  $Q_{DOB}$  here is a low-pass filter which makes the  $Q_{DOB}G_n^{-1}$  physically realizable. According to Fig. 2, the disturbance estimation is given by [2]

$$\hat{d} = Q_{DOB} [(\varepsilon + d)G_p G_n^{-1} - \varepsilon] . \quad (5)$$

In the cERL beam commissioning, this DOB control method is demonstrated by successfully compensating the beam-loading, as well as by successfully suppressing the power supply ripples and microphonics [2].

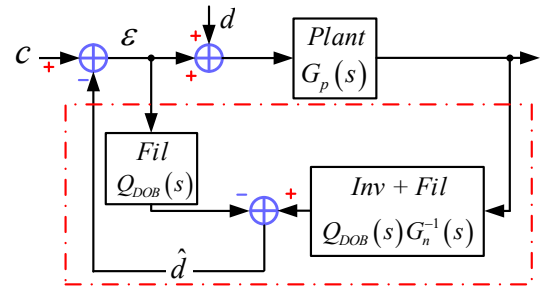


Figure 2: DOB control with  $Q$ -filter.

### COMBINED CONTROLLER

In our design, we incorporate the ILC algorithm, as well as DOB control with the traditional proportional (P) feedback controller. The overall control block diagram is given by Fig. 3. As discussed above, we have designed two types of ILC algorithm: P-type ILC and plant-inversion ILC in the combined controller. It should be mentioned that in the plant-inversion ILC case, the learning function  $L$  is not equal to  $G_n^{-1}$  any more. The overall system need to be considered and the ILC algorithm is modified by [5]

$$u_{j+1}^{ILC}(k) = Q_{ILC} [u_j^{ILC}(k) + T_u^{-1} e_j(k)] . \quad (6)$$

Where  $T_u$  represents the close loop transfer function matrix from the ILC control signal  $u_j^{ILC}$  to the plant output  $f(k)$ . The learning function is now defined as  $L = T_u^{-1}$ .

### EXPERIMENT ON CAVITY SIMULATOR

The control algorithm in Fig. 3 is demonstrated in a real-time cavity-simulator based test bench [9]. Main components of the simulator include cavity base-band models for fundamental mode and parasitic modes, a mechanical model of the LFD and model for beam current. The unpredictable disturbance model (e.g. microphonics) is also taken into account in our simulator. The cavity simulator is implemented in a field programmable gate array (FPGA) which is connected with digital LLRF systems. It is possible to test the function of the presented algorithms with the the cavity simulator in the absence of the real SC cavities. In the experiment, we select the cavity and RF parameters mainly based

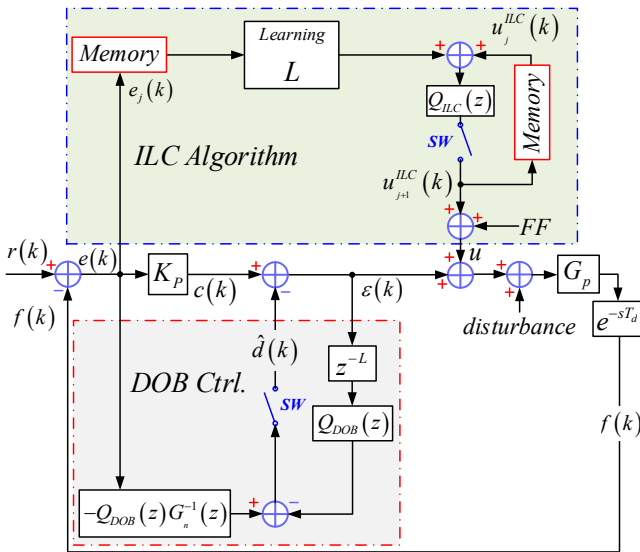


Figure 3: Overall model of "P+DOB+ILC" control. The presented ILC algorithm and DOB control are indicated by blue and red block, respectively.

on the KEK-STF project ( $Q_L \approx 4.6 \times 10^6$ , pulse duration  $\approx 1.65$  ms, repetition rate = 5 Hz).

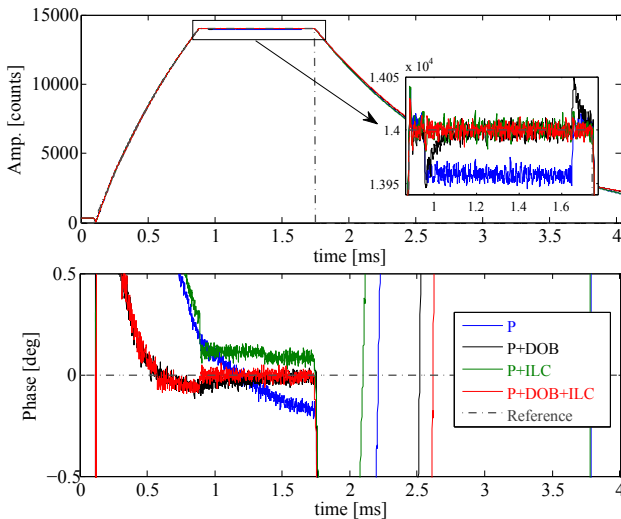


Figure 4: Comparison of P control (blue), "P+DOB" control (black), "P+ILC" control (green) and "P+DOB+ILC" control (red).

Figure 4 compares the cavity pick-up signal under four different control methods including traditional P control (blue), "P+DOB" control (black), "P+ILC" control (green) and "P+DOB+ILC" control (red). In the cavity simulator part, we have introduced a nearly on-crest beam current with  $\pm 10\%$  fluctuations, as a result, beam loading effects mainly appears in the amplitude of the pick up signal. In all of these four approaches, we maintain the P parameters same (loop gain  $\approx 150$ ). The beam loading effect and the microphonics is almost compensated by "P+DOB" control except in the head and end of the beam current. The main

reason is the limitation of the  $Q_{DOB}$  bandwidth in the DOB control. In the "P+ILC" case, there is a deviation in the phase due to the unpredictable microphonics and beam fluctuations. In the "P+DOB+ILC" case (red), the LFD and beam-loading effects is perfectly compensated, as well as the microphonics.

Figure 5 compares the convergence rate of the P-type ILC (blue) and plant inversion-based ILC (red). According to Fig. 5, the plant inversion-based ILC convergences at a faster rate than P-type ILC. This improvement is very important in a real beam operation.

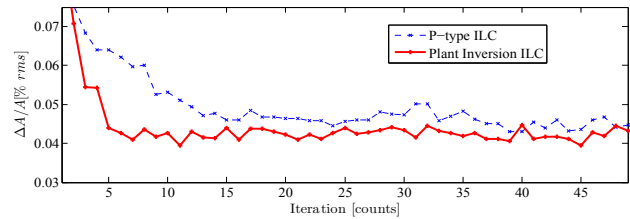


Figure 5: Comparison of convergence rate of the P-type ILC (blue) and plant inversion-based ILC (red).

## SUMMARY

We have presented a "P+DOB+ILC" control strategy that aims to reject both of the repetitive and unpredictable disturbances in LLRF system. Experiments on cavity simulator demonstrate that the stability of the LLRF system is improved after implementing the presented approach. We hope to extend these control strategy to the real pulse mode operated accelerators like STF and ILC.

## REFERENCES

- [1] ILC, "ILC Technical Design Report", <http://www.linearcollider.org/ILC/?pid=1000895>
- [2] F. Qiu *et al.*, "Application of disturbance observer-based control in low-level radio frequency system in a compact energy recovery linac at KEK", in *PRSTAB*, 18, 092801(2015).
- [3] C. Schmidt, Ph.D. thesis, Technische Universität Hamburg-Harburg, 2010.
- [4] Bristow, Douglas A *et al.*, "A survey of iterative learning control", *IEEE Control Systems* 26.3 (2006): 96-114.
- [5] Shu-Wen Yu, Ph.D. thesis, University of California, Berkeley, 2011.
- [6] H. Hayano, "Superconducting accelerator development at STF for ILC", in *Proc. 12th Annual Meeting of Particle Accelerator Society of Japan*, Tsuruga, Japan, Aug. 2015, pp. 164-168.
- [7] M. Uchiyama, "Formation of high speed motion pattern of mechanical arm by trial", in *Trans. Soc. Instrument Contr. Engineers*, vol. 14, no. 6, pp.706-712, 1978.
- [8] K. Ohishi, "Microprocessor controlled dc motor for load insensitive position servo system", in *IEEE Trans. Ind. Electron.*, Vol. 34, pp.44-49, 1987.
- [9] Tomasz Czarski *et al.*, "TESLA cavity modeling and digital implementation in FPGA technology for control system development", in *NIMA*, 548(3) (2005)